

Electron standing-wave observation in the Pd overlayer on Au(111) and Cu(111) surfaces by scanning tunneling microscopy

Takayuki Suzuki* and Y. Hasegawa†

Institute for Solid State Physics, the University of Tokyo 5-1-5 Kashiwa-no-ha, Kashiwa, Chiba 277-8581, Japan

Z.-Q. Li,‡ K. Ohno,§ Y. Kawazoe, and T. Sakurai

Institute for Materials Research, Tohoku University, 2-1-1 Katahira, Sendai, 980-8577, Japan

(Received 23 March 2001; published 3 August 2001)

Electron standing waves in monolayer-high Pd overlayers grown on the Au(111) and the Cu(111) surfaces were observed by low-temperature ultrahigh vacuum scanning tunneling microscopy. We found that the period of the oscillation in the Pd overlayers is longer than that of the clean surface of both Au(111) and Cu(111) substrates. The longer wavelength on the Pd overlayers is explained by an upward shift in energy level of the two-dimensional surface states.

DOI: 10.1103/PhysRevB.64.081403

PACS number(s): 73.20.At, 68.37.Ef, 73.61.At

It has been known that the (111) surface of noble metals, such as Au, Ag, and Cu, has surface-localized electronic states, which are confined by a projected band gap from the bulk side and an image potential from the vacuum side. The surface states, having an isotropic and nearly-free-electron-like (parabolic) energy dispersion, form an ideal two-dimensional (2D) electronic system. Since the states are localized in a few atomic layers on surfaces, surface defects, such as steps and adsorbates act as a scattering center for the electrons, producing standing wave patterns around them. Through direct observations of the electron standing waves (ESW's) using scanning tunneling microscopy (STM),^{1,2} various properties of the 2D electronic states^{3,4} and their interaction with surface steps,⁵⁻⁷ reconstructed structure,^{8,9} individual atoms,¹⁰⁻¹³ and molecules¹⁴ have been investigated.

Many studies have been performed on 2D electron systems localized at semiconductor interfaces of AlGaAs/GaAs and SiO₂/Si, and various interesting properties have been revealed, such as the quantum Hall effect, Wigner solid formation, electron wave interference effect and peculiar optical characteristics.¹⁵ One advantage 2D electron systems formed at semiconductor interfaces have is that an electron density in the system can be easily controlled by applying a voltage on a gate electrode and adjusting an electrostatic potential of the system. On the other hand, the electron density in the 2D surface states on metals, which is rather large compared with the ones at semiconductor interfaces, are not easily modified; it is basically an intrinsic material property, and thus what we can do is just choosing a proper one among materials. It would be particularly interesting if one could easily reduce and control the electron density of the metallic 2D electron system. Various unique phenomena would be elucidated using a local probe technique with an atomic-scale spatial resolution. So far, however, no established techniques for reducing the electron density have been reported, except one recently published by Park *et al.* on the Xe/Cu(111) system.¹⁶ One of the aims of the present study is to find and establish a method for reducing and controlling the electron density in order to study characteristics of the 2D surface electrons with an electron density as a parameter. Actually, photoemission electron spectroscopy (PES) studies were re-

ported on the energy-level variation of the surface states by alloy formation and alkali metal adsorption.¹⁷ We did not select these methods, because alloying and alkali metal adsorption would break coherency of electrons in the states and thus limit their mean free path, which is undesired for our purpose.

Pd(111) surface has surface states similar to those of Au(111) and Cu(111) surfaces but above the Fermi level.^{18,19} Since the surface states of Pd(111), as well as those of noble metals, decay into the bulk within a few monolayers, a Pd overlayer on the noble-metal surfaces produces surface states with an intermediate energy level between those of the two elements through interaction of wave functions of the two surface states. An energy level of surface states is thus shifted up from an original energy level of the substrate, resulting in a reduction of an electron density in the states. It is reported that palladium grows in a layer-by-layer manner on Cu(111) (Ref. 21) and Au(111) (Ref. 22) at the initial stage of growth (less than a few monolayers). Therefore, it is a good candidate for our purpose. In the present paper, we discuss standing wave observation and variation in wavelength on Pd overlayers grown on the Au(111) and the Cu(111) surfaces.

A low-temperature ultrahigh vacuum (LT-UHV) STM setup made by Unisoku Co. (USM type) was used in the present study. The base pressure in the STM chamber is about 2×10^{-8} Pa. In the STM, a specimen and a tip can be cooled with liquid helium down to 4.2 K. Au(111) samples were prepared by depositing gold on a cleaved mica at room temperature (RT) and successive annealing at about 500 °C. The Au deposition was done using a resistively heated tungsten filament with a thin Au wire. Cu(111) samples were prepared by cutting from a Cu single crystal. The samples were electrochemically etched in a cold solution of HNO₃ and methanol before introducing into the UHV chamber. The samples were cleaned in the UHV condition by a repetitive cycle of Ar⁺ sputtering and annealing at about 500 °C. Palladium was evaporated on Cu(111) at RT and on Au(111) at about 200 °C, using a resistively heated tantalum thin foil wrapping a Pd wire. Since palladium deposited on Au(111) surface at RT forms small multilayer islands nucleated at the

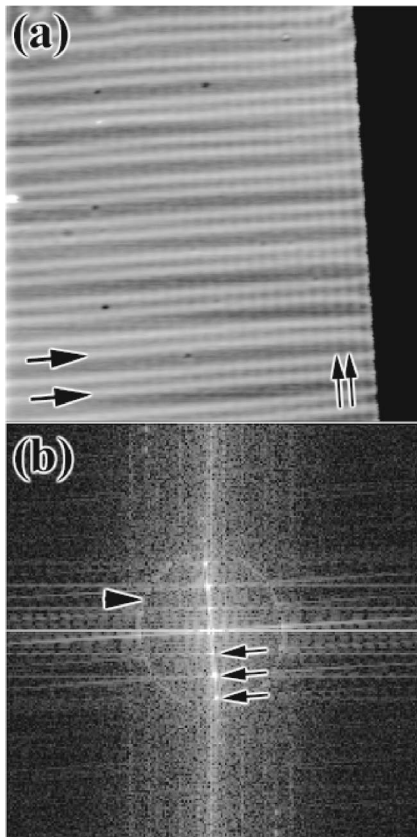


FIG. 1. (a) STM image of Au(111) surface. The size of observed area is $54 \text{ nm} \times 49 \text{ nm}$. It was taken with a bias voltage of 10 mV and a tunneling current of 0.1 nA . The temperature of the sample was 4.2 K . (b) Fourier-transformed (FT) pattern of the (a). A ring structure due to the electron standing waves and spots due to the $22 \times \sqrt{3}$ reconstructed structure are observed.

elbow site of the herringbone structure as described in a previous report,²² the substrates were heated during the deposition in order to restrict the nucleation and to make large islands. All STM observations were carried out at 4.2 K with a bias voltage of 10 mV and a tunneling current of 0.1 nA .

A typical STM image of a clean Au(111) surface is shown in Fig. 1(a) ($54 \text{ nm} \times 49 \text{ nm}$). A characteristic double-strip pattern due to the $22 \times \sqrt{3}$ reconstructed structure^{24,23,25} was observed on the terrace as indicated by large arrows in the lower left side of the image. There is a step on the right-hand side of the image, and electron standing waves (ESW's) due to scattering by the step are observed around it as indicated by small arrows in the lower right side of the image. Figure 1(b) shows a Fourier-transformed (FT) pattern of Fig. 1(a). Spots and a ring due to the reconstructed structure and the ESW were clearly seen as indicated by arrows and arrowheads, respectively. A period due to the ESW oscillation is measured to be $1.8 \pm 0.1 \text{ nm}$ from the FT pattern while a period of the reconstructed structure is 6.4 nm . Since the applied bias voltage is small (10 mV), the ESW's in the image correspond to those formed with surface states at the Fermi energy level. The period should thus be equal to the value of π/k_f , where k_f is the wave number of the surface states at the Fermi energy. Our measurement is consistent

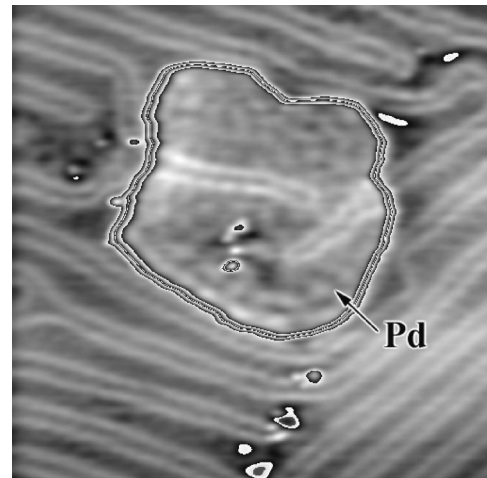


FIG. 2. An STM image of the Au(111) surface after Pd deposition ($70 \text{ nm} \times 63 \text{ nm}$, a bias voltage: 10 mV , a tunneling current: 0.1 nA , 4.2 K). Contrast of the image is adjusted so that fine structures on both Au substrate and monolayer-high Pd island are clearly resolved. Electron standing waves are clearly visible on the Pd island. The period of the waves is measured to be $3.5 \pm 0.4 \text{ nm}$.

with a value of k_f (1.7 nm^{-1}) measured by photoemission spectroscopy (PES) (Ref. 26) and the results of previous STM observations of ESW on this surface.^{1,8,9}

Figure 2 shows an STM image of the Au(111) surface after Pd deposition ($70 \text{ nm} \times 63 \text{ nm}$). The amount of Pd on the surface is estimated to be around 0.2 ML from STM observation. There is a monolayer-high Pd island in the middle of the image, as indicated by an arrow labeled with Pd. The ESW pattern is visible on the 2D Pd island, as well as two bright paired lines due to misfit dislocations. On the Au substrate, the ESW pattern is very weak because of the small reflection coefficient at the lower terrace.¹ The period of the ESW on the Pd island is measured to be $3.5 \pm 0.4 \text{ nm}$ from the FT pattern, longer than that of Au(111) surface.

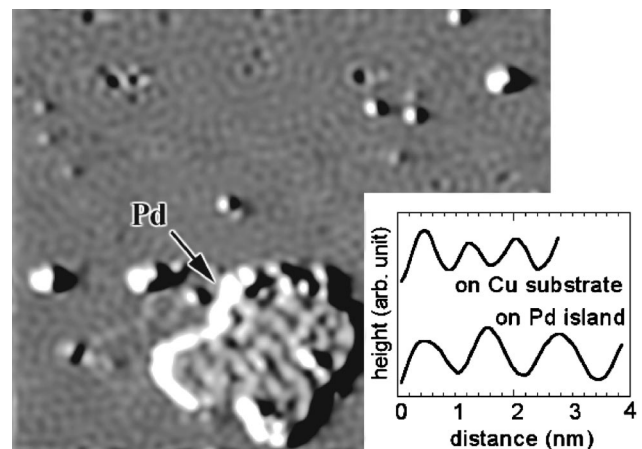


FIG. 3. An STM image (horizontal derivative) of the Cu(111) surface after Pd deposition ($54 \text{ nm} \times 41 \text{ nm}$, bias voltage: 10 mV , tunneling current: 0.1 nA , 4.2 K). Inset: apparent height profiles measured around an upper step edge of the Cu substrate and Pd overlayer.

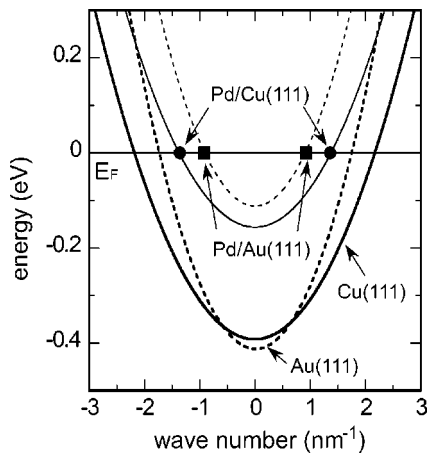


FIG. 4. An energy-dispersion curve of Au(111) (bold dotted line) and Cu(111) (bold solid line) surface states. The measured values of Fermi wave number on Pd/Au(111) (square) and Pd/Cu(111) (circle) are also plotted. The thin lines are an energy-dispersion curve crossing the data point of Fermi wave number on Pd/Au(111) (dotted line) and Pd/Cu(111) (solid line) surfaces with the same an effective mass as that of the substrate surface states.

Our observations on the Pd/Cu(111) system were similar to Pd/Au(111). Figure 3 shows an STM image of the Cu(111) surface after Pd deposition ($54 \text{ nm} \times 41 \text{ nm}$). In addition to several surface defects and small Pd clusters, a monolayer-high Pd island in the lower middle of the image is observed as indicated by an arrow labeled with Pd. On the Cu substrate the ESW pattern is clearly seen around the defects and the adsorbates. Its period is measured to be 1.4 nm, which is nearly the same as the previously reported value by PES (Ref. 26) and STM (Ref. 2) (1.5 nm). The ESW is also seen on the Pd island. The period on the Pd island is measured to be $2.3 \pm 0.3 \text{ nm}$, obviously larger than that observed on the Cu substrate.

In both cases, Pd/Au(111) and Pd/Cu(111) systems, Pd overlayer exhibits ESW with a larger period than those of the substrate, indicating it has surface states with a smaller wave number at the Fermi level. The measured wave number is plotted with the energy dispersion curve of Au(111) and Cu(111) surface states in Fig. 4. As is indicated with a fine line in the figure, the longer wavelength on Pd layers can be interpreted by an upward shift of energy level of surface states on the Pd overlayers. By assuming the same effective mass on the Pd overlayer as that of the substrate, the energy shift of the surface states is evaluated to be about 0.30 and 0.24 eV for the Au(111) and the Cu(111) surfaces, respectively.

As briefly mentioned above, the (111) surface of noble metals, as well as Pd, have localized electronic states, so-called Shockley states, with their center at the Γ point in an inverted L gap of the bulk states. With one less valence electron than noble metals, the electronic states of Pd are shifted upwards relative to those of noble metals. The unoccupied surface states of Pd are thus located at 1.3 eV above the Fermi energy,¹⁹ while those of Au and Cu are partially occupied (binding energy: 0.41 and 0.39 eV, respectively).²⁶ Wave functions of the surface states are localized in surface

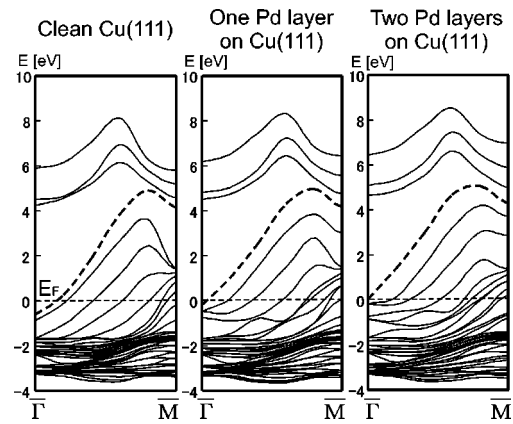


FIG. 5. Results of the first-principles total-energy calculations for Cu(111), monolayer Pd on Cu(111), and two layer Pd on Cu(111) systems. Dotted lines are calculated energy-dispersion curves of surface states. This figure demonstrates that energy level of the surface states is shifted upwards with Pd thickness on Cu(111) substrate.

layers, decaying into the bulk gap; the decay length estimated from a simple one-dimensional scattering model^{27,20} is about 0.9, 0.9, and 1.2 nm for the Au(111), Cu(111), and Pd(111) surfaces, respectively. Since these values are several times longer than monolayer thicknesses of these materials (0.236, 0.208, and 0.225 nm for the Au(111), Cu(111), and Pd(111), respectively), wave function of the surface states penetrate into a few layers from the surface. In a growth of Pd overlayer on Au or Cu(111) surface, one can thus expect that energy levels of surface states on Pd overlayer changes with its thickness from a level around that of the substrate at an initial stage to the intrinsic unoccupied level after a growth of layers thicker than the decay length.

According to the phase analysis model,²⁸ the energy level of Shockley surface states of noble metals is determined by the condition that the sum of phase shifts from bulk scattering (due to the band gap) and from the image potential should be equal to zero. In a case of system with an overlayer, a total phase shift including the one required for a round trip in the overlayer should be equal to 2π times an integer.²⁸ The energy range where the surface states are located (-0.5 to 0 eV with respect to the Fermi energy) corresponds to an energy level just below the lower edge $L_{2'}$ of the bulk Pd states, and thus the phase shift due to the monolayer-high overlayer is slightly smaller than 2π . Since both phase shifts due to the bulk band gap and image potential increase with an energy, energy level of surface states should be shifted up in order to compensate the phase loss due to the overlayer. Gradual variation of energy level is predicted for both Pd/Cu(111) and Au/Cu(111) systems based on the model.

This prediction is supported theoretically with the first-principles total-energy calculations employing ultrasoft pseudopotentials²⁹ for Cu and Pd systems, as is shown in Fig. 5. Slabs are used for modeling the surface with 8 bulk and 5 vacuum layers. The top and bottom atoms in the surface three layers are allowed to relax while the atoms in the center two layers are fixed in the bulk positions. Details of the calculated method will be published elsewhere.³⁰ Energy-

dispersion curves calculated for Cu(111) substrate, 1 monolayer (ML) Pd/Cu(111), and 2ML Pd/Cu(111) are plotted in Fig. 5. Dotted lines indicate the states localized on the surface layers. The results demonstrate that the surface states are formed near the Fermi level for 1ML Pd/Cu(111) and 2ML Pd/Cu(111) systems, as well as Cu(111) and that with a thickness of Pd layer the energy level of the surface states shifts to higher energy. The calculated results on 1ML Pd on Cu(111) are qualitatively consistent with the present experimental results. Note that an effective mass of Pd/Cu(111) surface states does not change from that of Cu(111) surface states although the effective masses of Pd(111) and Cu(111) surface states are quite different [$0.2m_0$ for Pd (Ref. 19) and $0.46 m_0$ for Cu (Ref. 26) where m_0 is a mass of electron]. We thus believe that our assumption of the same effective mass of Pd overlayer surface states as substrate is reasonable.

Neuhold and Horn³¹ reported a variation of energy levels in the Ag/Si(111) system and explained it with a strain accumulated on the surface layer. In the present cases, however, both Pd/Cu and Pd/Au show larger wavelength in spite of the fact that the opposite sign of strain is expected in the Pd

layer (tensile on Au and compressive on Cu). It does not seem that the strain has a significant effect on the wavelength or energy level of the surface states in the present cases. Further studies are, however, obviously required in order to solve this issue.

In conclusion, we have observed standing waves in Pd monolayers on Cu(111) and Au(111) surfaces, and found that their wavelengths are longer than those of the substrates. It can be explained by the up-shift in an energy level of the surface states in the Pd overlayers. By adjusting the element of material deposited and its thickness, one can modify and control electron density in the 2D surface states to some extent. This technique opens a way to elucidate unique characteristics of the 2D electron systems in a nanometer size spatial resolution.

T. Suzuki and Y.H. acknowledge T. Sasaki, H. Mizuno, K. Takeda, and T. Nagamura, Unisoku Co. for technical assistance and M. Ono for image processing. This work was partly supported by a Grant-in-Aid for Scientific Research (No. 12450020) from the Ministry of Education, Science, Sports, and Culture of Japan.

*Present address: Fritz-Haber-Institut der Max-Planck-Gesellschaft, Berlin, Germany.

[†]Author to whom correspondence should be addressed; e-mail: hasegawa@issp.u-tokyo.ac.jp

[‡]Present address: Steacie Institute for Molecular Sciences, National Research Council of Canada, Ottawa, Ontario, Canada.

[§]Present address: Faculty of Engineering, Yokohama National University, Yokohama, Japan.

¹Y. Hasegawa and Ph. Avouris, *Phys. Rev. Lett.* **71**, 1071 (1993).

²M.F. Crommie, C.P. Lutz, and D.M. Eigler, *Nature (London)* **363**, 524 (1993).

³J. Li, W.-D. Schneider, R. Berndt, O.R. Bryant, and S. Crampin, *Phys. Rev. Lett.* **81**, 4464 (1998).

⁴L. Burgi, O. Jeandupeux, H. Brune, and K. Kern, *Phys. Rev. Lett.* **82**, 4516 (1999).

⁵Ph. Avouris and I.-W. Lyo, *Science* **264**, 942 (1994).

⁶L. Burgi, O. Jeandupeux, A. Hirstein, H. Brune, and K. Kern, *Phys. Rev. Lett.* **81**, 5370 (1998).

⁷J. Li, W.-D. Schneider, R. Berndt, and S. Crampin, *Phys. Rev. Lett.* **80**, 3332 (1998).

⁸D. Fujita, K. Amemiya, T. Yakabe, H. Nejoh, T. Sato, and M. Iwatsuki, *Phys. Rev. Lett.* **78**, 3904 (1997).

⁹W. Chen, V. Madhavan, T. Jamneala, and M.F. Crommie, *Phys. Rev. Lett.* **80**, 1469 (1998).

¹⁰M.F. Crommie, C.P. Lutz, and D.M. Eigler, *Science* **262**, 218 (1993).

¹¹V. Madhavan, W. Chen, T. Jamneala, M.F. Crommie, N.S. Zeller, P.H. Dederichs, and J. Wingreen, *Science* **280**, 567 (1998).

¹²J. Li, W.-D. Schneider, R. Berndt, and B. Delley, *Phys. Rev. Lett.* **80**, 2893 (1998).

¹³J. Repp, F. Moresco, G. Meyer, K.-H. Rieder, P. Hyldgaard, and M. Persson, *Phys. Rev. Lett.* **85**, 2981 (2000).

¹⁴S.J. Stranick, M.M. Kamna, and P.S. Weiss, *Science* **266**, 99

(1994); M.M. Kamna, S.J. Stranick, and P.S. Weiss, *ibid.* **274**, 119 (1996).

¹⁵J.H. Davies, *The Physics of Low-Dimensional Semiconductors* (Cambridge University Press, Cambridge, 1998).

¹⁶Ji-Yong Park, U.D. Ham, S.-J. Kahng, Y. Kuk, K. Miyake, K. Hata, and H. Shigekawa, *Phys. Rev. B* **62**, R16341 (2000).

¹⁷T.C. Hsieh, T. Miller, and T.-C. Chiang, *Phys. Rev. Lett.* **55**, 2483 (1985); T.C. Hsieh and T.-C. Chiang, *Surf. Sci.* **166**, 544 (1986).

¹⁸M. Pessa and O. Jylha, *Solid State Commun.* **46**, 419 (1983).

¹⁹A. Schäfer, I.L. Shumay, M. Wiets, M. Weinelt, Th. Fauster, E.V. Chulkov, V.M. Silkin, and P.M. Echenique, *Phys. Rev. B* **61**, 13 159 (2000).

²⁰Th. Fauster and W. Steinmann, in *Electromagnetic Waves: Recent Developments in Research, Vol. 2: Photonic Probes of Surfaces*, edited by P. Halevi (Elsevier, Amsterdam, 1995), Chap. 8.

²¹Y. Hasegawa, J.F. Jia, K. Inoue, A. Sakai, and T. Sakurai, *Surf. Sci.* **386**, 328 (1997).

²²A.W. Stephenson, C.J. Baddeley, M.S. Tikhov, and R.M. Lambert, *Surf. Sci.* **398**, 172 (1998).

²³D.D. Chambliss, R.J. Wilson, and S. Chiang, *Phys. Rev. Lett.* **66**, 1721 (1991); *J. Vac. Sci. Technol. B* **9**, 928 (1991).

²⁴Ch. Wöll, S. Chiang, R.J. Wilson, and P.H. Lippel, *Phys. Rev. B* **39**, 7988 (1989).

²⁵J.V. Barth, H. Brune, G. Ertl, and R.J. Behm, *Phys. Rev. B* **42**, 9307 (1990).

²⁶S.D. Kevan and R.H. Gaylord, *Phys. Rev. B* **36**, 5809 (1987).

²⁷S.G. Davison and M. Steslicka, *Basic Theory of Surface States* (Clarendon Press, Oxford, 1992).

²⁸N.V. Smith, *Phys. Rev. B* **32**, 3549 (1985); Th. Fauster, *Appl. Phys. A* **59**, 639 (1994).

²⁹D. Vanderbilt, *Phys. Rev. B* **41**, 7892 (1990); G. Kresse and J. Furthmüller, *ibid.*, **54**, 11169 (1996).

³⁰Z.-Q. Li, K. Ohno, and Y. Kawazoe (unpublished).

³¹G. Neuhold and K. Horn, *Phys. Rev. Lett.* **78**, 1327 (1997).